

Fast Control Latency Uncertainty Elimination for BESIII ETOF Upgrade*

Yun Wang(汪昫)^{1,2}, Ping Cao (曹平)^{1,2;1)}, Shu-bin Liu (刘树彬)^{1,3}, Qi An (安琪)^{1,2}

¹State Key Laboratory of Particle Detection and Electronics, University of Science and Technology of China, Hefei, 230026, China

²School of Nuclear Science and Technology, University of Science and Technology of China, Hefei 230027, China

³Department of Modern Physics, University of Science and Technology of China, Hefei 230027, China

Abstract: A new fanning topology is proposed to precisely fan out fast control signals in Beijing Spectrometer (BES III) End-cap Time of Flight (ETOF) electronics. However, uncertainty in transfer latency is introduced by the new fanning channel, which will degrade the precision of fast control. In this paper, latency uncertainty elimination for BESIII ETOF upgrade is introduced. The latency uncertainty is determined by a Time-Digital-Converter (TDC) embedded in Field-Programmable Gate Array (FPGA) and is eliminated by re-capturing at synchronous and determinate time. Compared with the existing method of Barrel-cap TOF (BTOF), it has advantages of flexible structure, easy calibration and good adaptability. Field tests on BES III ETOF system show that this method eliminates transfer latency uncertainty effectively.

Key words: Transfer latency uncertainty, SerDes, BES III, Endcap TOF

PACS: 29.85.Ca

1 Introduction

The Beijing Electron Positron Collider (BEPC) and the Beijing Spectrometer (BES) were upgraded to BEPC II and BES III respectively in the summer of 2008. To further improve the overall time resolution of the Particle Identification (PID), the End-cap time of flight (ETOF) is upgraded with newly developed MRPC detectors [1,2,3]. After upgrade, the total time resolution will be improved from 138ps to about 80ps [4]. To achieve this specification, new readout electronics for ETOF should be developed.

In the existing BESIII TOF system, there are 2 VME crates, each of which has a fast control module (FCTL) inside receiving signals from the fast control system (FCS). For new ETOF electronics, two extra new VME crates are added to adapt the large amount of MRPC channels. However, there are only two critical and calibrated channels between FCS and the TOF sub-system. New topology needs to be proposed for transmitting fast control signals to new ETOF electronics.

There are several different methods to transmit fast control signals in particle experiments. In Barbar experiment, fast control signal is transmitted through electric cables without being encoded [5]. There is no transmission latency uncertainty in this experiment. In LHC, fast control signal is transmitted through dedicated ASIC chip designed by CERN [6]. The transmission latency uncertainty is eliminated by special technique of encoding and synchronizing code [7]. In BESIII, fast control signal is distributed with technique of serializing and de-serializing (SerDes) [8]. Fast control signals are encoded from 8bit to 10bit data with timing information and then serialized into bit stream at the transmitting side for output. However, at the receiver side, there might be 10 discrete phases when recovering clock from the bit stream. These 10 phases lead to latency uncertainty in distributing fast control signals. In BESIII FCS design, the fast

control data is re-synchronized at determinate time to avoid the area of uncertainty [8,9]. This method succeeds only when the length of the distributing channels are equal. However, two extra newly brought VME crates change the distributing topology for ETOF fast control signals, which leads to the failure of existing method. In this paper, a new method is presented. This method utilize a TDC to calculate the uncertainty area automatically. It is easy to be used and can be carried out automatically.

2 Fast Control Latency Uncertainty in ETOF upgrade

2.1 Structure after upgrade

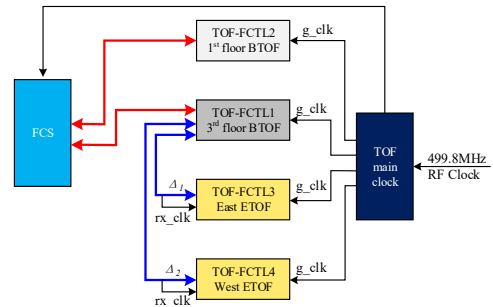


Fig. 1 Structure for fast control signal fanning out after ETOF upgraded

There are several sub-systems such as TOF, Muon, MDC, EMC connected to the BESIII FCS [8]. FCS resides in the BES III trigger system. Inside FCS, there are totally five fiber channels dedicated for fanning fast control signals (L1 trigger signal, fiber reset signal etc.) out to one sub-detector system. For TOF fast control sub-system, there are 4 electronic modules (TOF-FCTL1~4 in Fig. 1) for receiving signals distributed from FCS. As shown in Fig. 1, two for ETOF and two for BTOF respectively. There are two clocks on each ETOF fast control module,

* Funded by CAS maintenance project for major scientific and technological infrastructure (IHEP-SW-953/2013)

1) E-mail: cping@ustc.edu.cn

one is the global clock (g_clk) distributed from TOF main clock, the other is the rx_clk recovered from the bit stream (blue lines in Fig. 1) sent from BTOF. The phase difference between these two clocks is noted as Δ .

In order to avoid modifications of the existing FCS structure, there are only two fiber channels (red lines in Fig. 1) left for TOF-FCTL. In ETOF electronics, there are two extra new VME crates, which need two additional fiber channels. In Fig. 1, to distribute fast control signals to all TOF-FCTL modules, the module residing in the 3rd floor BTOF crate acts as a router. It receives fast control signals from FCS and then fans them out to each ETOF module. Two extra channels (blue lines in Fig. 1) are added in the new distributing topology.

2.2 Uncertainty introduced by SerDes

The existing FCS uses TLK1501 [10] to distribute fast control signals to all sub-systems. The same technique is used in ETOF module design for compatibility purpose. The basic principle for using the technique of SerDes is that the transmitter sends encoded data according to a reference clock, while the receiver acquires data according to the clock recovered from the transmitted bit stream. So the acquired data is aligned to the recovered clock. In Fig. 2, yellow signal denotes the transmitting reference clock, while the green one denotes the recovered clock. Unfortunately, each time the SerDes powers up, there is uncertainty in the phase of recovered clock as shown in Fig. 2, where the oscilloscope runs in persistence mode. This uncertainty is not a problem for traditional communication applications, where the correctness of data is the key point. However, for BESIII FCS distributing fast control signals, the most critical point is the time of fast control signal being recognized.

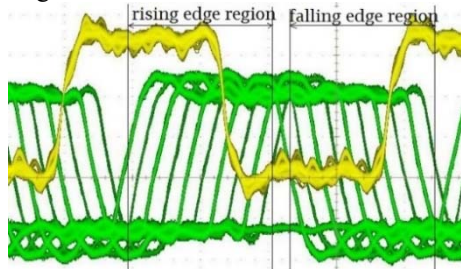


Fig. 2 Phase uncertainty in the recovered clock.

For BESIII, the clock period is 24ns. The recovery clock has ten phases, which are uniformly spaced in the 10.2ns range. As the work clock of the TOF-FCTL is the global clock, the recovery data must be re-synchronized by the global clock. Because the phase difference Δ might take any value, the rising edge of the global clock might lie in the rising edge region of the recovery clock. The transfer latency will have one cycle (24ns) difference between the first recovery clock phase and the last one.

In the existing BTOF module, the encoded fast control data capturing time is postponed to avoid the unstable area (responding to the uncertain recovered clock) in data bus according to the global synchronous clock, not the recovered clock [8,9]. The transmitted data is re-captured by the global synchronous clock which is shifted by a DLL with configurable delay ability. This can succeed in the

existing TOF sub-system based upon two facts. Firstly, there is a global precise clock network everywhere in BESIII electronics. Secondly, there are only two same distributing channels (red lines in Fig. 1) from FCS to TOF sub-system, which means the acquiring time can be easily calibrated and adjusted. During calibration, FCS and TOF are placed in the same place and both are set into debugging mode. FCS continuously sends trigger data to TOF. At the TOF side, it is convenient to adjust the delay value by comparing the transmitted and received trigger signal with an oscilloscope.

Unfortunately the existing method cannot be applied in ETOF upgrade, as the manual field test is very hard. ETOF electronics should have the ability to eliminate latency uncertainty automatically in the field of spectrometer.

3 Uncertainty Elimination

3.1 Principle description

Because of the uncertainty in the recovered clock (rx_clk) at the receiver side, there is an unstable period in the fast control data which is recovered according to the rx_clk . This unstable period is 1.2ns less than a half cycle as area P or N shown in Fig. 3. The rx_clk has the same frequency as the global synchronous clock, so if the recovered data is sampled at both edges of a reference clock (shifted from the TOF global clock, abbreviated as ref_clk), at least one value is reliable. Fig. 3 shows the timing graph where the rx_data (16-bit width) is aligned with rx_clk .

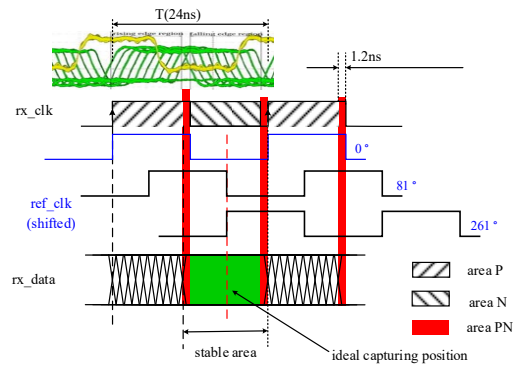


Fig. 3 Timing graph for elimination principle

One of ref_clk 's edge (leading or trailing) must be in the stable area of rx_data . To improve the reliability of data capturing, the middle position (red dash line in Fig. 3) is the ideal capturing position, which makes the capture margin large enough. Furthermore, this position is determinate and does not change whenever SerDes powers up. Supposing there is no skew between rx_clk and ref_clk ($\Delta=0$ in Fig. 1), if fixing the position of rx_clk and then checking that of ref_clk , there will randomly distribute 10 phases, among which both 81° (falling edge) and 261° (rising edge) correspond to this ideal position (bold black lines shown in Fig. 3).

The problem left is to obtain the clock with phase 81° (or 261°). Actually, this finding process can be considered as checking the relative position between rx_clk and

ref_clk equivalently. There's no need to exactly distinguish each position among these 10 phases. The principle is to make the real capturing position move to the ideal position as near as possible. So the relative phase difference can be measured by a TDC with bin size of 3ns. One clock cycle (T) can be divided into 8 parts with initial phase value from ϕ_0 to ϕ_7 , where $\phi_i=i*45^\circ$. If the TDC's dynamic range is only one cycle (T), it will generate 8 data (0~7) corresponding to each phase respectively (Fig. 4).

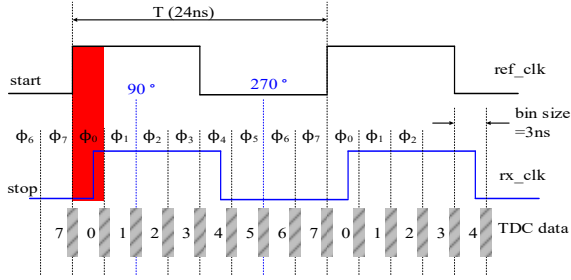


Fig. 4 TDC data and clock phase

In Fig. 4, the rising edge of ref_clk is used to start the TDC counting, while the rising edge of rx_clk is used to stop it. If the phase difference is less than one bin size (red block in Fig. 4), the TDC will give an output value of 0. So according to the output code from TDC, it is easy to know the relative position between rx_clk and ref_clk. However, because the existence of clock jitter or bit dis-matching of rx_data (16-bit width), TDC may generate two values randomly during the critical period of bin transition (gray block in Fig. 4). For the case of 0 phase difference, TDC can generate 0 or 7, while for the case of 90° , the data is 1 or 2.

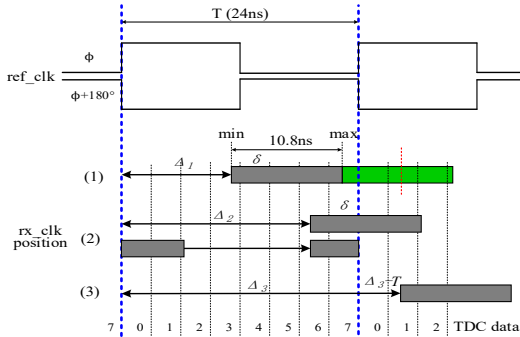


Fig. 5 Algorithm for finding rx_data re-capture position

Because of the existence of uncertainty in rx_clk phase, the phase difference between ref_clk and rx_clk can be considered as following:

$$\Delta\phi = \Delta + \delta$$

Δ denotes the difference caused by signal distribution channel (blue lines in Fig. 1), and δ denotes the uncertainty caused by SerDes.

In Fig. 5, dark grey blocks denote the uncertain area where the rising edge of rx_clk occurs. The width of this area is 10.8ns. The center of the attached area (green block in Fig. 5) is the ideal position for data capturing. There are three possibilities for phase difference (Δ) discussed as following:

(1) $0 \leq \Delta < T/2 + 1.2$

The position of rx_clk rising edge swings in one period T as shown in Fig. 5. TDC generates the following data:

- {0, 1, 2, 3, 4} when Δ is digitized as 0;
- {1, 2, 3, 4, 5} when Δ is digitized as 1;
- {2, 3, 4, 5, 6} when Δ is digitized as 2;
- {3, 4, 5, 6, 7} when Δ is digitized as 3.

(2) $T/2 + 1.2 \leq \Delta < T$

The position of rx_clk rising edge overflows outside one period T as shown in Fig. 5. TDC generates the following data:

- {4, 5, 6, 7, 8}, when Δ is digitized as 4;
- {5, 6, 7, 8, 9}, when Δ is digitized as 5;
- {6, 7, 8, 9, 10}, when Δ is digitized as 6;
- {7, 8, 9, 10, 11}, when Δ is digitized as 7.

Since the TDC dynamic range is only one cycle, the swing area (from TDC output data) will be folded back to the beginning of this cycle. So the data pair generated by TDC is:

- {4, 5, 6, 7, 0}, when Δ is digitized as 4;
- {5, 6, 7, 0, 1}, when Δ is digitized as 5;
- {6, 7, 0, 1, 2}, when Δ is digitized as 6;
- {7, 0, 1, 2, 3}, when Δ is digitized as 7;

Compared with the first situation, the $\langle \min, \max \rangle$ value pair is definitely $\langle 0, 7 \rangle$ whichever value Δ is.

(3) $\Delta > T$

It can be classified into case 1 or 2 if the TDC counting start signal is switched to the next following rising edge of ref_clk until $(\Delta - n * T) < T$.

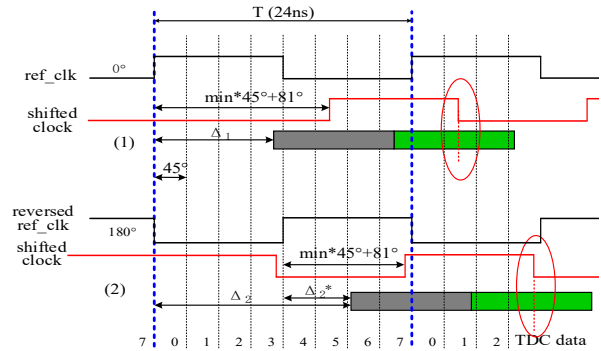


Fig. 6 Selection of capturing rx_data (green blocks denote the stable area for rx_data) at shifted clock colored with red

According to the above mentioned discussion, the algorithm for re-capturing rx_data at the receiving side is listed as following:

- (1) Receiver resets SerDes periodically to generate rx_clk with uncertain phase and set $rf=0$.
- (2) Measure the phase difference ($\Delta < T$, normalized to one cycle) between rx_clk and ref_clk, and count the min and max value to form $\langle \min, \max \rangle$ pair as well.
- (3) If $\langle \min, \max \rangle$ pair is not $\langle 0, 7 \rangle$, shift ref_clk with phase $(\min * 45^\circ + 81^\circ)$ and then go to step (5).
- (4) If $\langle \min, \max \rangle$ pair is $\langle 0, 7 \rangle$, shift ref_clk with phase 180° , $rf=1$ and then go back to step (2).
- (5) Capture rx_data with the shifted ref_clk ($rf=0$) or reversed ref_clk ($rf=1$) at its falling edge (red circle in Fig. 6) and then go to step (6).
- (6) Finish.

3.2 Implementation

Fig. 7 is the block diagram of uncertainty elimination algorithm implemented in FPGA. The recovered data (rxd with 16-bit width) is directly fed into a group of flip flops

inside one common logic array block (LAB) in FPGA for data alignment. It is synchronized to rx_clk . Then the aligned data is sampled by two groups of flip-flops simultaneously, one works on phase ϕ , the other works on $\phi+180^\circ$ (ϕ is automatically obtained through the phase difference measuring flow and the resolution of phase shifting is 200ps). The two groups of flip-flops must be constrained together to ensure that the 16-bits aligned data are sampled under the same condition. After being synthesized and implemented in FPGA, timing analysis shows that the data skew of all the sample DFFs is only a few picoseconds. Finally, one of the sampled data is selected as the stable output according to the above mentioned algorithm.

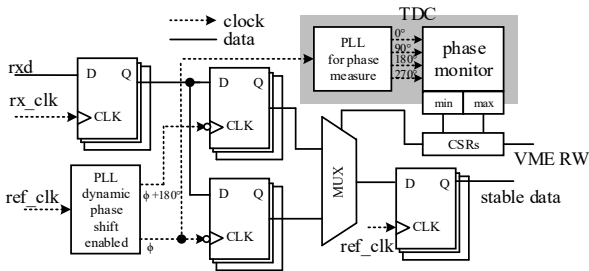


Fig. 7 Logic block diagram for uncertainty elimination

The sampling ref_clk phase can be adjusted by logic automatically. A multi-phase clock interpolation technique based TDC [11] implemented in FPGA is used to measure the phase differences of rx_clk and ref_clk . Fig. 8 is the schematic of the TDC. Because the phase difference is less than one clock period (24ns), the TDC does not need large dynamic range and the TDC structure can be further simplified. The TDC contains four parts as shown by the attached blocks in Fig. 8. The ϕ clock (also shown in Fig. 7) is the main clock for the TDC. The $df_clk[3:0]$ is generated by doubling the frequency of the ϕ clock and shifting the phases from 0° to 270° respectively. The hit signal is generated by dividing the ref_clk by a factor of two. Each sample block generates two bits. All these bits are arranged and synchronized by the ϕ clock to generate the output $v[7:0]$. As the period of hit is twice as the ϕ clock, the TDC generate one output every two clock cycles. The phase

monitor (shown in Fig. 7) calculates the maximum and minimum value of v continuously.

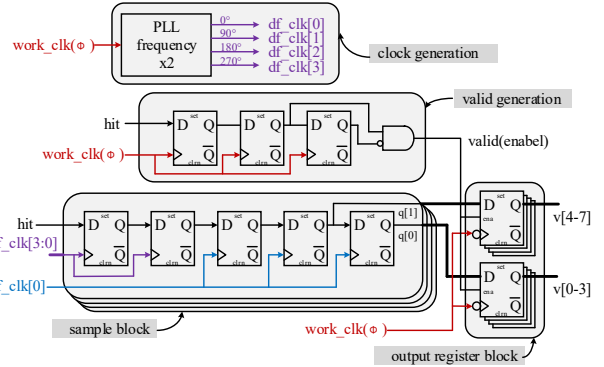


Fig. 8 The schematic of the TDC

Fig. 4 has shown the characteristic of this TDC. The performance has been measured by an indirect way. The test is executed in the following steps:

- (1) Enable the TLK1501 to generate stable rx_clk .
- (2) Enable the TDC module to start measurement for one minute.
- (3) Record the measured $\langle min, max \rangle$ pair. Disable the TDC module to clear the $\langle min, max \rangle$ value.
- (4) Shift the ϕ clock with 200ps. If the total phase shift reaches one cycle (24ns i.e. 120 steps), then go to step (5). If not, go to step (2).
- (5) Finish.

Fig. 9 is the recorded data. Fig. 9 (a) and (c) show that each bin contains about 15 shift steps, which span $15 \times 0.2ns = 3ns$. The linearity is good. The Fig. 9 (b) shows that at most one shift step has nonzero (max-min) value at each bin transition boundary. This indicates that the transition area (diagonal areas in Fig. 4) is in the range less than $2 \times 200ps = 400ps$ including all contributions (such as clock jitter, hit jitter, DFF setup and hold time requirements). As the phase monitor does statistics on the output and the 400ps transition region is far less than 3ns bin size, it will have no substantial effect on the methods proposed in section 3.1.

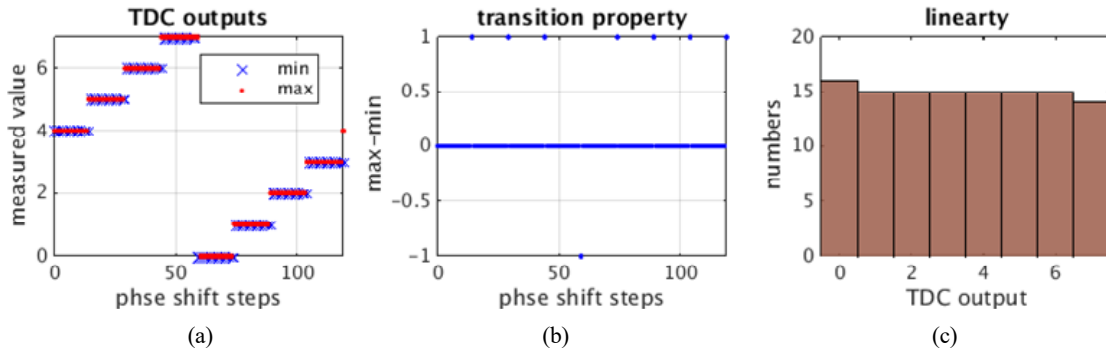


Fig. 9 The measured property of the TDC. (a) is the output versus shift steps; (b) draws the differences between max value and min value.;(c) shows the linearity of the TDC.

If the SerDes is triggered into the cycle of being enabled and disabled continuously, it will generate rx_clk with

uncertain phase. The phase difference (Δ) can be measured by the phase monitor.

uncertainty for BESIII ETOF upgrade can be eliminated successfully.

Acknowledgement

We gratefully acknowledge Dr. Hongliang Dai, Zhi Wu, Xiaolu Ji, Jingzhou Zhao, Xiaozhuang Wang and other members of BESIII ETOF upgrade group of IHEP for their earnest support and help during the beam test.

1 E Cerron-Zeballos, J Choi, D Hatzifotiadou et al, Nucl. Instrum. Methods A, 434(2):362-372(1999)
2 H. F. Chen, C. Li, X. L. Wang et al. High Energy Physics and Nuclear Physics, 26(3):201-206(2002)(in Chinese)
3 J. Wu, B. Bonner, H. F. Chen et al. Nucl. Instrum Methods A, 538:243-248(2005)
4 H. H. Fan, C. Q. Feng, W. J. Sun et al, IEEE Trans. Nucl. Sci., 60(5):3563-3569(2013)
5 https://www.slac.stanford.edu/BFROOT/www/Detector/DAQ/Fast_Cntrl_Tim_System/fcts3_0.ps, retrieved 24th March 2016
6 J. Christiansen, A. Marchioro, P. Moreira et al. Receiver ASIC for timing, trigger and control distribution in LHC experiments, in Nuclear Science Symposium and Medical Imaging Conference Record, edited by E. Barsotti. Piscataway (USA: San Francisco, 1995), p. 597-601

7 B.G. Taylor, IEEE Trans. Nucl. Sci., 45(3): 821-828(1998)
8 K. Wang, Design of BESIII Trigger Fast Control System, Ph.D. Thesis(HeiFei: University of Science and Technology of China, 2006)(in Chinese)
9 X. Z. Liu, S. B. Liu, W. Zheng et al, Journal of Jilin University, 38(2):483(2008)(in Chinese)
10 <http://www.ti.com/lit/ds/symlink/tlk1501.pdf>, retrieved 24th March 2016
11 C. F. Ye, L. Zhao, S. B. Liu et al. Rev. Sci. Instrum, 85(4): 045115(2014)